Donor-Ligand-Substituted Cyclopentadienylchromium(III) Complexes: A New Class of Alkene Polymerization Catalyst. 2. Phosphinoalkyl-Substituted Systems

Arno Döhring, Vidar R. Jensen,* Peter W. Jolly,* Walter Thiel, and Jan C. Weber[1]

Max-Planck-Institut für Kohlenforschung, Kaiser-Wilhelm-Platz 1, D-45470 Mülheim an der Ruhr, Germany

Received February 22, 2001

A series of phosphinoalkyl-substituted cyclopentadienylchromium complexes, e.g., (η^1:η^5-$R_2PC_2H_4C_5H_4$)$CrCl_2$, have been synthesized. The complexation of the P atom to the chromium has been confirmed by crystal structure determinations. Activated by methylalumoxane (MAO), these compounds catalyze the oligomerization and polymerization of ethylene. The catalytic activity and the degree of oligomerization are controlled by the steric properties of the substituents on the donor atom: the smaller the substituent, the greater the activity and the lower the molecular weight of the oligomer. Density functional calculations indicate that propagation and termination through β-hydrogen transfer are competitive for small substituents and that the latter process, which involves spin inversion, becomes selectively disfavored with increasing size of the substituents. For large substituents β-hydrogen elimination to the chromium atom is found to be the preferred route for termination, although this reaction is less facile than insertion.

Introduction

Recently we reported that highly active, homogeneous catalysts for the polymerization of ethylene under mild conditions can be generated by activating amino-substituted cyclopentadienyl chromium(III) complexes, e.g., (η^1:η^5-$R_2NC_2H_4C_5Me_4$)$CrCl_2$, with methylalumoxane.[2,3] We have now extended these investigations to the related phosphinoalkyl-substituted analogue and have observed a remarkable dependence of the product composition of the reaction with ethylene upon the steric properties of the substituent (R) on the P atom. A preliminary account of this work has been published.[4,5]

Results and Discussion

Although η^1:η^5-phosphinoalkyl-substituted cyclopentadienyl derivatives have been prepared for many of the transition metals,[6] e.g., Mn, Ru, and Rh, examples involving chromium were not known prior to our investigations.[7] These compounds can be prepared by reacting the alkali metal salt of the ligand with Cr-$(THF)_3Cl_3$, and their accessibility depends on the ease of preparation of the cyclopentadienyl derivative.

Preparation of the Phosphinoalkyl-Substituted Cyclopentadienyl Derivatives. The synthetic routes available have been reviewed.[6] Most easily prepared are the $R_2PC_2H_4C_5H_4Li$ (**1a**−**1l**) and $R_2PC_2H_4$IndenylLi (**2a**−**2c**) species which may be formed in good yield by reacting the appropriate lithium phosphide with spiro-[2.4]hepta-4,6-diene[8] or spiro[cyclopropane-1,1′-indene][9] (eqs 1 and 2).

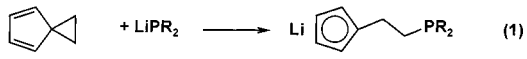

(1)

1 a, R=Me; **b**, R=Et; **c**, R=Pr; **d**, R=^{i}Pr; **e**, R=^{i}Bu; **f**, R=^{t}Bu; **g**, R=Neopentyl; **h**, R=Hexyl; **i**, R=Cy; **j**, R=Ph; **k**, R=o-Tolyl; **l**, R=1-Naphthyl

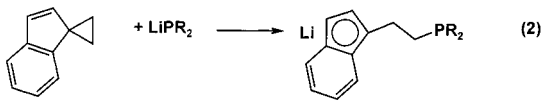

(2)

2 a, R=Et; **b**, R=^{i}Bu; **c**, R=Cy

The related 3-phosphinopropyl-substituted derivatives (**3**, **4**) may be prepared by reacting $R_2PC_3H_6Cl$ with

(1) Part of the Ph.D. Thesis submitted to Ruhr-Universität Bochum in 1999.
(2) Döhring, A.; Göhre, J.; Jolly, P. W.; Kryger, B.; Rust, J.; Verhovnik, G. P. J. *Organometallics* **2000**, *19*, 388.
(3) Jensen, V. R.; Angermund, K.; Jolly, P. W.; Børve, K. J. *Organometallics* **2000**, *19*, 403.
(4) Döhring, A.; Jensen, V. R.; Jolly, P. W.; Thiel, W.; Weber, J. C. In *Organometallic Catalysts and Olefin Polymerization*; Blom, R., Follestad, A., Rytter, E., Tilset, M., Ystens, M., Eds.; Springer-Verlag, 2001; p 127.
(5) Döhring, A.; Jensen, V. R.; Jolly, P. W.; Thiel, W.; Weber, J. C. *Macromol. Symp.*, in press.
(6) Butenschön, H. *Chem. Rev.* **2000**, *100*, 1527.
(7) Jolly, P. W.; Jonas, K.; Verhovnik, G. P. J.; Döhring, A.; Göhre, J.; Weber, J. C. (Studiengesellschaft Kohle m.b.H.) WO-A 98/04570, 1998 [*Chem. Abstr.* **1998,** *128*, 167817v].
(8) Wilcox, C. F.; Craig, R. R. *J. Am. Chem. Soc.* **1961**, *83*, 3866.
(9) Kauffmann, T.; Berghus, K.; Rensing, A.; Ennen, J. *Chem. Ber.* **1985**, *118*, 3737.

10.1021/om010146m CCC: $20.00
Publication on Web 05/01/2001

Table 1. Phosphinoalkyl-Substituted Cyclopentadienylchromium Dichloride Compounds

compound	yield (%)	anal.: found (calcd) C	H	Cl	Cr	P
$(Me_2PC_2H_4C_5H_4)CrCl_2$ (**7a**)	13	39.3 (39.2)	5.0 (5.1)	25.5 (25.7)	18.7 (18.8)	11.2 (11.2)
$(Et_2PC_2H_4C_5H_4)CrCl_2$ (**7b**)	40	43.6 (43.4)	6.1 (6.0)	23.3 (23.3)	17.2 (17.1)	10.1 (10.2)
$(Pr_2PC_2H_4C_5H_4)CrCl_2$ (**7c**)	84	46.9 (47.0)	6.7 (6.7)	21.3 (21.3)	15.8 (15.7)	9.3 (9.3)
$(^iPr_2PC_2H_4C_5H_4)CrCl_2$ (**7d**)	59	46.8 (47.0)	6.6 (6.7)	21.2 (21.3)	15.4 (15.7)	9.2 (9.3)
$(^iBu_2PC_2H_4C_5H_4)CrCl_2$ (**7e**)	64	50.2 (50.0)	7.2 (7.3)	19.7 (19.7)	14.5 (14.4)	8.5 (8.6)
$(^tBu_2PC_2H_4C_5H_4)CrCl_2$ (**7f**)	22	49.9 (50.0)	7.3 (7.3)	19.6 (19.7)	14.6 (14.4)	8.5 (8.6)
$(Neopentyl_2PC_2H_4C_5H_4)CrCl_2$ (**7g**)	68	52.7 (52.6)	8.1 (7.7)	17.4 (18.3)	12.9 (13.4)	− (8.0)
$(Hexyl_2PC_2H_4C_5H_4)CrCl_2$ (**7h**)	39	54.6 (54.8)	8.3 (8.2)	17.1 (17.0)	12.6 (12.5)	7.4 (7.4)
$(Cy_2PC_2H_4C_5H_4)CrCl_2$ (**7i**)	85	55.2 (55.4)	7.3 (7.3)	17.1 (17.2)	12.7 (12.6)	7.7 (7.5)
$(Ph_2PC_2H_4C_5H_4)CrCl_2$ (**7j**)	quant	57.2 (57.0)	4.5 (4.5)	17.9 (17.7)	12.7 (13.0)	7.6 (7.7)
$(Ph_2PC_2H_4C_5H_4)CrCl_2$·Tol (**7j′**)	84	63.4 (63.4)	5.4 (5.3)	14.4 (14.4)	10.5 (10.6)	6.2 (6.3)
$(o\text{-}Tolyl_2PC_2H_4C_5H_4)CrCl_2$ (**7k**)	13	58.7 (58.9)	5.0 (5.2)	16.5 (16.6)	11.9 (12.1)	7.1 (7.2)
$(1\text{-}Naphthyl_2PC_2H_4C_5H_4)CrCl_2$ (**7l**)	quant	64.7 (64.8)	4.4 (4.4)	14.2 (14.2)	10.3 (10.4)	6.2 (6.2)
$(1\text{-}Naphthyl_2PC_2H_4C_5H_4)CrCl_2$·$Me_2CO$(**7l′**)	17	64.4 (64.5)	5.1 (5.1)	12.7 (12.7)	9.2 (9.3)	5.6 (5.6)
$(Et_2PC_2H_4Indenyl)CrCl_2$ (**8a**)	61	50.7 (50.9)	5.6 (5.1)	20.2 (20.0)	14.5 (14.7)	8.8 (8.7)
$(^iBu_2PC_2H_4Indenyl)CrCl_2$ (**8b**)	81	55.7 (55.6)	6.9 (6.9)	17.2 (17.3)	12.8 (12.7)	7.5 (7.6)
$(Cy_2PC_2H_4Indenyl)CrCl_2$ (**8c**)	23	59.9 (59.8)	7.1 (7.0)	15.3 (15.3)	11.2 (11.3)	6.6 (6.7)
$(Cy_2PC_3H_6C_5H_4)CrCl_2$ (**9a**)	31	56.2 (56.3)	7.7 (7.6)	16.7 (16.6)	12.1 (12.2)	7.4 (7.3)
$(Ph_2PC_3H_6C_5H_4)CrCl_2$ (**9b**)	73	58.1 (58.0)	5.0 (4.9)	17.1 (17.1)	12.4 (12.6)	7.3 (7.5)
$(Cy_2PC_3H_6Indenyl)CrCl_2$ (**10**)	9	60.3 (60.5)	7.1 (7.2)	15.0 (14.9)	10.8 (10.9)	6.7 (6.5)
$(Ph_2PC_3H_6C_5Me_4)CrCl_2$ (**11**)	27	61.1 (61.3)	6.1 (6.0)	15.0 (15.1)	10.8 (11.1)	6.4 (6.6)

NaCp/BuLi[10] or IndenylLi (eqs 3 and 4).

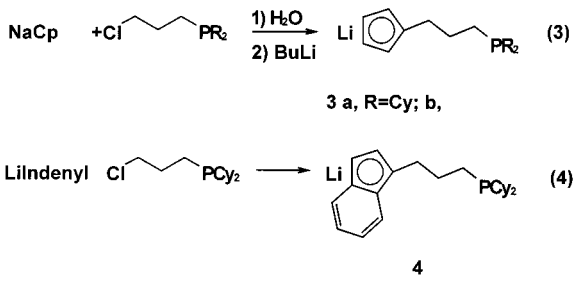

The lithium salt of 3-tetramethylcyclopentadienylpropyl-1-diphenylphosphine (**5**) was prepared in a multistep published procedure starting from tetramethylcyclopent-2-enone (eq 5).[11]

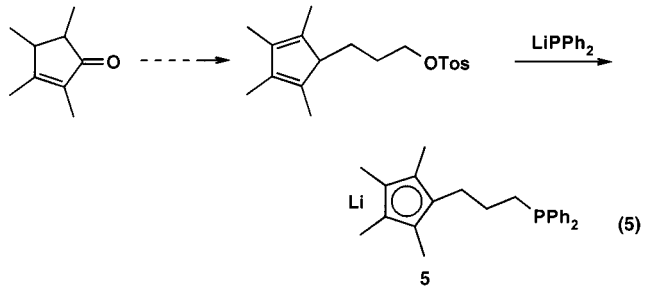

In addition, $Cy_2AsC_2H_4C_5H_4Li$ (**6**) has been prepared by reacting the lithium arsenide with spiro[2.4]hepta-4,6-diene (eq 6).[12]

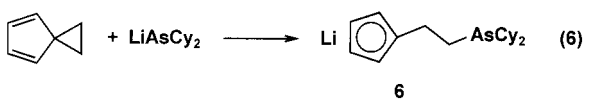

(10) Kettenbach, R. T.; Bonrath, W.; Butenschön, H. *Chem. Ber.* **1993**, *126*, 1657.
(11) Bensley, D. M.; Mintz, E. A.; Sussangkarn, S. J. *J. Org. Chem.* **1988**, *53*, 4417.
(12) Kauffmann, T.; Berghus, K.; Ennen, J. *Chem. Ber.* **1985**, *118*, 3724.

Scheme 1. Preparation of the Organochromium Compounds

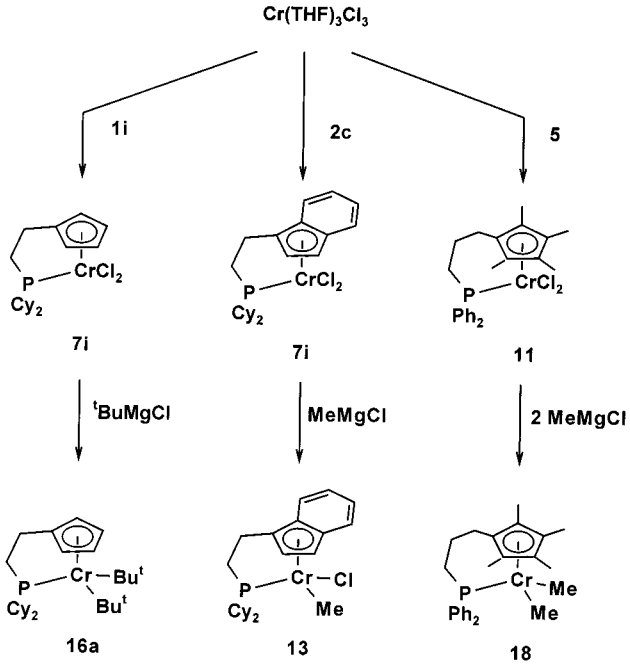

Preparation and Structure of the Organochromium Compounds. The phosphinoalkyl-substituted cyclopentadienylchromium dichloride compounds, **7**−**11**, were prepared by reacting the appropriate lithium salt with $Cr(THF)_3Cl_3$ in THF (examples are shown in Scheme 1). The compounds are thermally stable at room temperature, and the monosubstituted derivatives (**7** and **9**) can even be handled briefly in the air. The indenyl derivatives **8** and **10** are dark green, whereas the monosubstituted cyclopentadienyl species and the tetramethyl-substituted compound **11** are dark blue. The analytical data for the isolated compounds are listed in Table 1.

For mechanistic purposes, we have also prepared a number of chromium-alkyl derivatives (**12**−**18**) by reacting the dichloride species with a Grignard reagent or MeLi (Scheme 1), and the analytical data for these

Table 2. Phosphinoalkyl-Substituted Cyclopentadienylchromium Alkyl Compounds

compound	yield (%)	anal.: found (calcd) C	H	Cr	P
$(Cy_2PC_2H_4C_5H_4)Cr(Et)Br$ (**12**)[a]	24	56.2 (56.0)	8.0 (7.8)	11.6 (11.5)	6.9 (6.9)
$(Cy_2PC_2H_4Indenyl)Cr(Me)Cl$ (**13**)[b]	17	65.2 (65.2)	7.9 (8.0)	11.9 (11.8)	6.9 (7.0)
$(Et_2PC_2H_4C_5H_4)CrMe_2$ (**14**)	22	59.4 (59.3)	9.3 (9.2)	19.6 (19.8)	11.7 (11.8)
$(Cy_2PC_2H_4C_5H_4)CrMe_2$ (**15a**)	49	67.8 (67.9)	9.6 (9.8)	14.2 (14.0)	8.4 (8.3)
$(Cy_2PC_2H_4C_5H_4)Cr^tBu_2$ (**15b**)	13	71.0 (71.2)	10.6 (10.6)	11.5 (11.4)	7.0 (6.8)
$(Ph_2PC_2H_4C_5H_4)CrPr_2$ (**16a**)	59	71.9 (72.3)	7.9 (7.7)	12.5 (12.5)	7.6 (7.5)
$(Ph_2PC_2H_4C_5H_4)Cr^tBu_2$ (**16b**)	22	73.1 (73.1)	8.1 (8.2)	11.7 (11.7)	7.3 (7.0)
$(Ph_2PC_2H_4C_5H_4)CrCy_2$ (**16c**)	26	75.2 (75.1)	8.1 (8.1)	10.4 (10.5)	6.4 (6.3)
$(Cy_2PC_3H_6C_5H_4)CrMe_2$ (**17**)	45	68.4 (68.5)	10.0 (9.9)	13.5 (13.5)	8.0 (8.0)
$(Ph_2PC_3H_6C_5Me_4)CrMe_2$ (**18**)	2	72.9 (72.7)	8.2 (8.0)	11.4 (11.1)	7.4 (7.2)

[a] Br analysis: 17.7 (17.7). [b]Cl analysis: 8.1 (8.0).

Table 3. Selected Structural Data for Phosphinoalkyl- and Arsinoalkyl-Substituted Cyclopentadienylchromium Compounds[a]

	7i	**7j′**	**9a**	**11**[b]	**15a**	**19**
			Interatomic Distances (Å, esd)			
Cr−D1	1.886	1.887	1.890	1.888	1.926	1.885
Cr−P1	2.459(1)	2.447(1)	2.460(1)	2.472(1)	2.450(1)	2.537(1)[c]
Cr−Cl1	2.276(1)	2.273(1)	2.294(1)	2.284(1)	2.058(5)[d]	2.277(1)
Cr−Cl2	2.279(1)	2.291(1)	2.284(1)	2.284(1)	2.083(4)[d]	2.282(1)
P−C1	1.850(3)	1.821(3)	1.834(4)	1.837(3)	1.845(3)	1.968(3)[c]
P−C(R)[e]	1.845(2)	1.813(3)	1.847(4)	1.818(1)	1.841(3)	1.971(3)[c]
P−C′(R)[e]	1.844(2)	1.826(3)	1.855(4)	1.822(3)	1.841(3)	1.966(3)[c]
C1−C2	1.531(4)	1.536(5)	1.515(6)	1.520(5)	1.531(5)	1.537(5)
C2−C3	1.501(4)	1.505(5)	1.512(7)	1.513(5)	1.518(5)	1.512(5)
C3−C4			1.506(7)	1.512(5)		
			Bond Angles (deg)			
Cl1−Cr−Cl2	95.9(1)	98.7(1)	98.8(1)	97.7(1)	90.4(2)[d]	96.9(1)
P1−Cr−Cl1	98.3(1)	94.4(1)	94.6(1)	94.1(1)	100.1(1)[d]	99.9(1)[c]
P1−Cr−Cl2	102.2(1)	99.1(1)	95.5(1)	94.0(1)	102.9(1)[d]	97.2(1)[c]
P1−Cr-D1	109.8	110.1	117.5	119.6	110.2	109.6[c]
C1−P1−Cr	104.3(1)	100.7(1)	108.2(1)	108.0(1)	103.6(1)	102.7(1)[c]
C1−P−C(R)[e]	105.5(1)	104.3(1)	105.7(2)	105.8(1)	105.0(2)	104.7(1)[c]
C1−P−C′(R)[e]	106.7(1)	107.7(1)	105.8(2)	104.1(2)	105.0(1)	106.3(1)[c]
C(R)−P−C′(R)[e]	105.4(1)	104.3(1)	107.4(2)	102.3(1)	105.0(1)	104.4(1)[c]

[a] See Figures 1 and 2 for the numbering of the atoms. D1 denotes the center of the Cp ring. [b]Data for one of the two independent molecules. [c]As atom. [d]Cr−CH_3. [e]P-bonded C atom of the substituent R.

are listed in Table 2. In contrast to the dichloride compounds, the dialkyl species are readily oxidized and are thermally less stable. All attempts to convert these species into ionic compounds of potential mechanistic relevance by reacting, for example, $(Cy_2PC_2H_4Indenyl)$-Cr(Me)Cl (**13**) with $NaBPh_4$ or $(Cy_2PC_2H_4C_5H_4)CrMe_2$ (**15a**) with $B(C_6F_5)_3$ were unfortunately unsuccessful.

For comparison purposes, one dialkylarsino-substituted cyclopentadienyl derivative was prepared (**19**, eq 7), and this was converted into the corresponding dimethyl derivative (**20**) by reaction with MeMgCl.

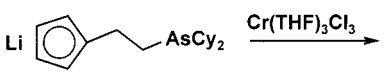

6

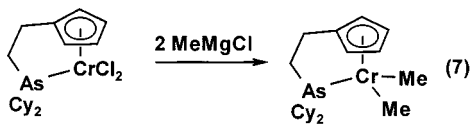

19 20

In contrast to the aminoalkyl-substituted cyclopentadienyl analogue,[2] the infrared spectra of the phosphinoalkyl-substituted species provide no readily interpretable information on the bonding situation at the donor atom, and since these Cr(III) compounds are paramagnetic (the high-spin configuration with three unpaired electrons has been confirmed using a superconducting quantum interference device (SQUID) for **7i** and **15a**), structural information is based upon crystal structure investigations of selected compounds. The molecular structures of **7i**, **7j′**, **9a**, **11**, and **15a** are shown in Figures 1 and 2 along with that of $(Cy_2AsC_2H_4C_5H_4)CrCl_2$ (**19**), and selected bond lengths and bond angles are listed in Table 3.

The crystal structures confirm that in all cases the donor atom is bonded to the chromium atom (Cr−P 2.45−2.47 Å). A comparison of the data for **7i** and **7j′** indicates that an increase in the steric requirements of the substituent (R) on the phosphorus atom is accompanied by a lengthening of the P−Cr bond (2.447(1) Å **7j′**; 2.459(1) Å, **7i**), while the (R)C−P−C(R) angle increases (104.3(1)°, **7j′**; 105.4(1)°, **7i**). The compounds **7i** and **9a** differ only in the length of the "spacer" between ring and donor atom, and the less strained arrangement in **9a** results in an increase in the (R)C−P−C′(R) angle (107.4(2)°, **9a**; 105.4(1)°, **7i**) and is accompanied by an increase in the Cl1−Cr−Cl2 angle (98.8(1)°, **9a**; 95.9(1)°, **7i**). These changes, however, have no effect upon the Cr−P bond length (2.46 Å, **7i/9a**).

The exchange of the Cl atoms in **7i** by Me groups in **15a** leads to a small decrease in the Cr−P bond length (2.450(1) Å, **15a**; 2.459(1) Å, **7i**) and in a significant increase in the separation (Cr−D) from the cyclopen-

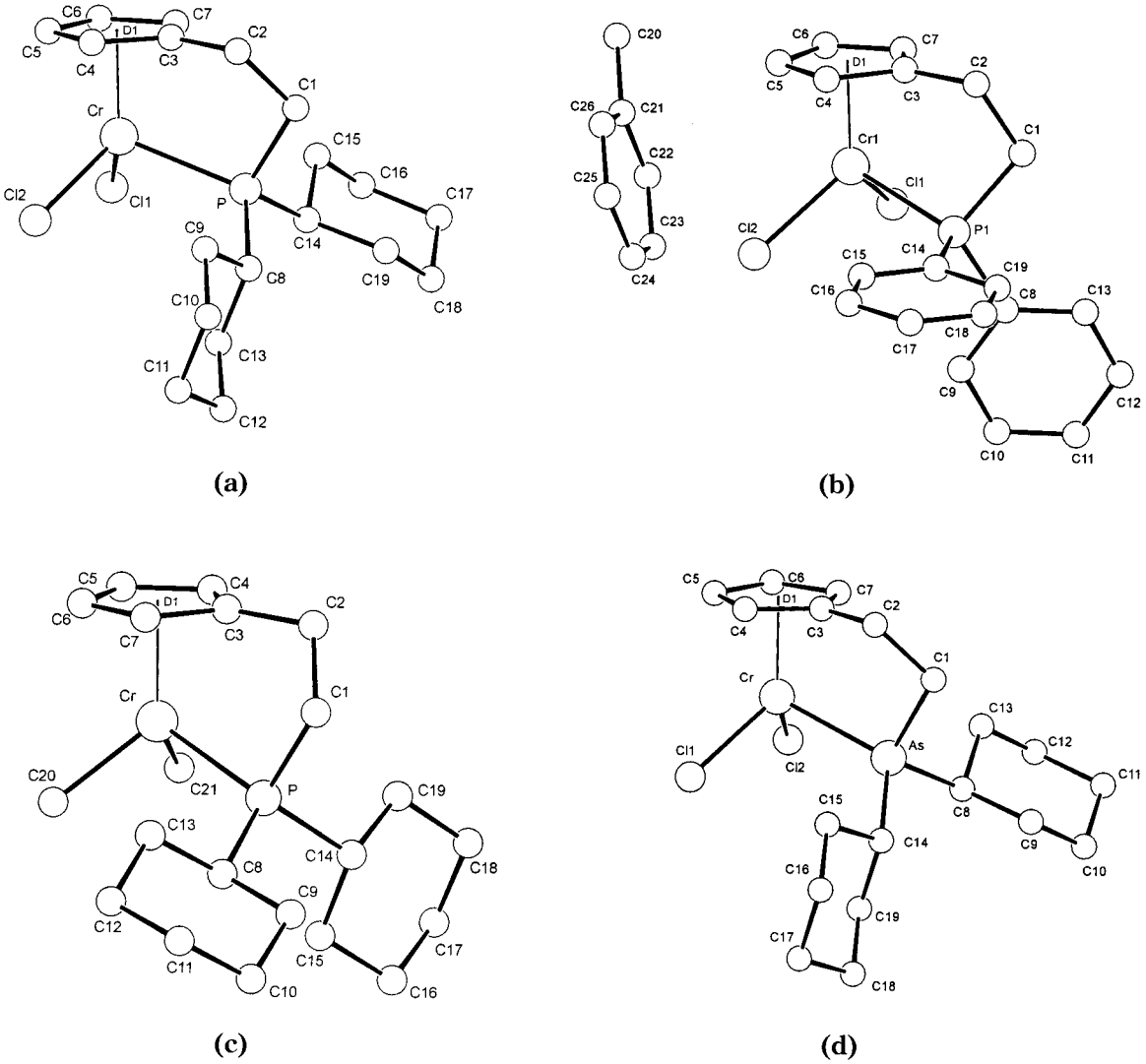

Figure 1. Molecular structures of (a) $(Cy_2PC_2H_4C_5H_4)CrCl_2$ (**7i**), (b) $(Ph_2PC_2H_4C_5H_4)CrCl_2$.Toluene (**7j′**), (c) $(Cy_2PC_2H_4C_5H_4)$-$CrMe_2$ (**15a**), and (d) $(Cy_2AsC_2H_4C_5H_4)CrCl_2$ (**19**).

tadienyl ring (1.926 Å, **15a**; 1.886 Å, **7i**) as a result of the increase in the electron density at the metal atom. Although the Cr−Me bonds in **15a** are significantly shorter than the Cr−Cl bonds in **7i** (2.058(5)/2.083(4) Å, **15a**; 2.276(1)/2.279(1) Å, **7i**), the difference in the electrostatic properties of the two substituents shows itself in the difference between the Cl−Cr−Cl angle (95.9(1)°) and the Me−Cr−Me angle (90.4(1)°).

The increase in the Cr-donor atom bond length upon exchanging the P-donor atom for an As-donor atom (2.459(1) Å, **7i**; 2.537(1) Å, **19**) is the result of the difference in the atomic radii (1.33 Å, As; 1.23 Å, P).

Catalytic Oligomerization and Polymerization of Ethylene. The organochromium compounds described in the preceding section were prepared in order to compare their catalytic behavior, in the presence of methylalumoxane (MAO), toward ethylene with that of the amino-substituted cyclopentadienyl chromium complexes described earlier.[2] The latter invariably convert ethylene into linear polyethylene having a molecular weight of 1−3 million with an activity that can be influenced by introducing substituents into the ring.

We confine our attention here to the behavior of the monosubstituted phosphinoalkylcyclopentadienylchromium catalysts of the general formula $(R_2PC_2H_4C_5H_4)$-$CrCl_2$ since these species are relatively easy to prepare and variation of the substituent R is unproblematic. To facilitate comparison, the catalyses were carried out under standard conditions in toluene at room temperature and at a constant pressure of 2 bar. Near isothermal conditions ($\Delta T = 3-4$ °C) were obtained by adjusting the concentration of the catalyst. The reaction was terminated after 4 min by simultaneously stopping the flow of ethylene into the reactor and injecting propanol to destroy the catalyst. These conditions are by no means optimal and considerably higher activities can be obtained by increasing the MAO concentration, by raising the temperature, and by changing the solvent. These effects as well as those of introducing substituents into the cyclopentadienyl ring will be discussed in a subsequent publication.

The product of the oligomerization was analyzed as three fractions: lower oligomers, nondistillable higher oligomers soluble in toluene, and solid polyethylene. The composition of the lower oligomer mixture has been determined by gas chromatography. An investigation of the composition of the soluble, higher oligomer fraction is in progress and will be reported separately: initial

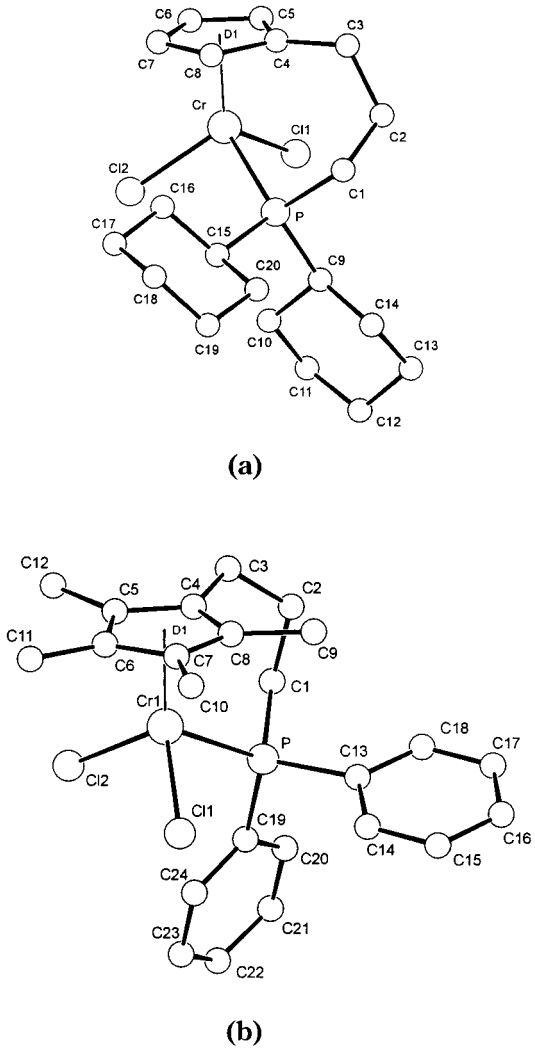

Figure 2. Molecular structures of (a) $(Cy_2PC_3H_6C_5H_4)CrCl_2$ (**9a**) and (b) $(Ph_2PC_3H_6C_5Me_4)CrCl_2$ (**11**).

Table 4. $(R_2PC_2H_4C_5H_4)CrCl_2$–MAO-Catalyzed Oligomerization and Polymerization of Ethylene[a]

R	product composition (%)[b]	activity[c]	$\theta(PR_3)$[d] (deg)
Me	C_4 (83.6), C_6 (13.0), C_{6+}(3.5)	4620	118
Et	C_4 (21.2), C_6 (26.3), C_8–C_{14} (47.7), C_{14+} (5.0)	4480	132
^{i}Bu	C_4 (10.6), C_6 (12.5), C_8–C_{14} (43.3), C_{14+} (33.6)	4230	143
^{i}Pr	C_6–C_{10} (3.1), PE (96.9, M_w 6.3 × 10^4)	3590	160
Cy	C_6–C_{10} (3.1), PE (96.9, M_w 1.8 × 10^5)	1450	170
^{t}Bu	C_4–C_8 (15.6), PE (84.4, M_w 1.3 × 10^5)	590	182
Ph	C_6–C_{10} (10.3), C_{12}–C_{14} (8.6), C_{14+} (76.7), PE (2.1)	5140	145
o-Tolyl	C_6–C_{10} (4.5), PE (95.5)	2330	194

[a] Standard condition: solvent, toluene; $P(C_2H_4)$ = 2 bar; Cr: MAO = 1:100; t = 4 min; T = 21 °C, ΔT = 4 °C. [b] C_4, 1-butene; C_6, 1-hexene etc.; reproducibility ± 2%. [c] kg product/mol Cr·h. [d] Tolman cone angle.

NMR investigations indicate that it consists exclusively of terminal olefins. The results are summarized in Table 4.

As can be seen from Table 4, both the catalytic activity and the degree of oligomerization are dependent upon the size of the substituents on the P atom: the larger the substituent, the lower the activity and the higher the degree of oligomerization. That these effects are mainly steric in origin is apparent from a comparison with the cone angle (θ) of the related triorganophosphine (PR_3) compounds as defined by Tolman[13] (Table 4), and this is underlined by the results for the phenyl- and *o*-tolyl-substituted derivatives.

An effect as dramatic as that described here has not been reported previously for a chromium catalyst. However, it should be mentioned that the polymerization of ethylene using MAO-activated diimine complexes of nickel[14] and pyridinediimine complexes of iron and cobalt[15–18] having aryl substituents, e.g., **21** and **22**, can be tailored to give long-chain oligomers by decreasing the size of the ortho-substituents on the aryl groups.

21

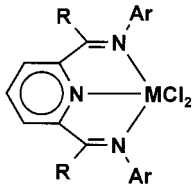

22 (M=Fe,Co)

In addition, it has been reported that the degree of oligomerization of ethylene catalyzed by $(\eta^3\text{-}C_3H_5)Ni(PR_3)\text{-}X\text{–}Et_3Al_2Cl_3$ is controlled by the nature of the tertiary phosphine bonded to the nickel atom: the main product with PMe_3 is the dimer, while in the presence of $P^tBu_2\text{-}^i$Pr higher oligomers are formed.[19] Finally, it has recently been shown that the classical SHOP ethylene oligomerization catalyst (**23**)[20] can be transformed into a polymerization catalyst (**24**) by introducing a salicylaldimine ligand having bulky groups in the ortho-position of the ligand.[21]

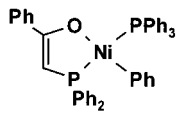

23

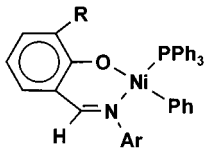

24

Of particular technical interest in our case is presumably the formation of a 1-butene/1-hexene mixture when R is methyl, of the mixture of long-chain oligomers when R is phenyl or isobutyl, and of polyethylene when R is cyclohexyl: the dimer/trimer mixture could be copolymerized directly with ethylene to low-density polyethylene, while the waxlike higher olefin mixture could form the basis of a chromium-catalyzed alternative to the SHOP process.

(13) Tolman, C. A. *Chem. Rev.* **1977**, *77*, 313.
(14) Killian, C. M.; Johnson, L. K.; Brookhart, M. *Organometallics* **1997**, *16*, 2005.
(15) Bennett, A. M. A. *Chemtech* **1999**, *29*, 24.
(16) Britovsek, G. J. P.; Bruce, M.; Gibson, V. C.; Kimberley, B. S.; Maddox, P. J.; Mastroianni, S.; McTavish, S. J.; Redshaw, C.; Solan, G. A.; Strömberg, S.; White, A. J. P.; Williams, D. J. *J. Am. Chem. Soc.* **1999**, *121*, 8728.
(17) Small, B. L.; Brookhart, M. *J. Am. Chem. Soc.* **1998**, *120*, 7143.
(18) Britovsek, G. J. P.; Mastroianni, S.; Solan, G. A.; Baugh, S. P. D.; Redshaw, C.; Gibson, V. C.; White, A. J. P.; Williams, D. J.; Elsegood, M. R. J. *Chem.-Eur. J.* **2000**, *6*, 2221.
(19) Bogdanović, B. *Adv. Organomet. Chem.* **1979**, *17*, 105.
(20) Vogt, D. *Appl. Homogen. Catal. Organomet. Cpds.* **1996**, *1*, 245.
(21) Younkin, T. R.; Connor, E. F.; Henderson, J. I.; Friedrich, S. K.; Grubbs, R. H.; Bansleben, D. A. *Science* **2000**, *287*, 460.

Table 5. Calculated Enthalpies and Free Energies (kcal/mol) for the Species Shown in Figure 3, Relative to Ethylene + $[(R_2DC_2H_4C_5H_4)CrPr]^+$, (I$\beta$(^{4}A))[a]

	D = P				D = N	
	R = Me		R = ^{t}Bu		R = Me	
species	ΔH_{298}	ΔG_{298}	ΔH_{298}	ΔG_{298}	ΔH_{298}	ΔG_{298}
Iγ(^{4}A) + ethylene[b]	7.4	7.5	8.8	8.4		
Iβ(^{4}A) + ethylene[b]	0.0	0.0	0.0	0.0	0.0	0.0
Iα(^{4}A) + ethylene[b]	8.5	7.2	6.4	5.7		
[Iα→IV]‡(^{4}A)[c]	8.4	13.0	9.3	17.8		
IV(^{4}A)	−2.5	8.7	4.0	15.5	0.1	10.4
[IV→VIγ]‡(^{4}A)	4.0	16.5	8.9	21.6	4.8	17.1
IVβ(^{2}A)	−3.7	11.1	11.4	26.5	10.3	24.2
[IVβ→Vβ]‡(^{2}A)	1.4	16.8	19.2	34.6	13.7	28.0
[Iβ→II]‡(^{4}A) + ethylene	8.9	9.1	10.1	11.2		
II(^{4}A) + ethylene	8.5	8.1	10.6	10.9	10.1	9.6
[II→III]‡(^{4}A) + ethylene[d]	31	28	29	25	31	26
III(^{4}A) + ethylene + propene	33.8	21.5	30.8	18.7	32.8	20.1

[a] From single-point total energies at optimized geometries, with zero-point energies and temperature corrections; see Computational Details. [b] Interconversion between different agostic conformers of **I** is facile ($\Delta G^‡_{298}$ < 11 kcal/mol for R = Me). [c] Ethylene coordination to β- or γ-agostic complexes is less favorable. A very shallow minimum assignable to a charge-induced dipole metal-ethylene complex is located prior to **[Iα→IV]‡(^{4}A)**. The thermochemical data for this complex have been omitted since they are not important for the discussion. [d] Entropic barrier estimated by stepwise geometry optimization and vibrational analysis; see Computational Details.

That the high activity of many of the catalysts and the product distribution are a consequence of the attachment of the donor ligand to the cyclopentadienyl ring is emphasized by the results with a $CpCr(PMe_3)Cl_2$−MAO catalyst: under the same standard conditions used for the $(Me_2PC_2H_4C_5H_4)CrCl_2$−MAO catalyst, an activity of only 120 kg product/mol Cr·h is observed, and moreover the product is polyethylene.[22] Low activity has also been reported for the $(C_5Me_5)Cr(PMe_3)Me_2$−MAO system, and in this case it has been suggested that the termination step involves chain transfer from chromium to aluminum.[23,24]

Mechanistic Considerations. The remarkable dependence of the product composition in the Cr-catalyzed reactions presented above upon the size of the substituents on the P-donor atom prompted us to investigate theoretically the mechanism of the reaction in the hope of obtaining insight into the origin of this effect.

In recent years, density functional theory (DFT) has become the method of choice for the computational investigation of the mechanisms of transition metal catalyzed olefin polymerization reactions (see for example refs 3, 25−27). In the present investigation we have selected a gradient-corrected functional (BPW91) in combination with DZP basis sets for geometry optimization and TZD2P basis sets for single-point energy evaluations; see Computational Details.

Two catalyst systems derived from **7a** (R = Me) or **7f** (R = ^{t}Bu), which span the product distribution from predominantly short oligomers to long-chain polyethylene, were selected for the computational investigations, and the results have been compared to those obtained with $(Me_2NC_2H_4C_5H_4)CrCl_2$, which has already been shown to generate polyethylene.[2] Although the active species for these systems has not been isolated, we assume that it is an alkylchromium cation generated by reacting the chromium dichloride compound with methylalumoxane (MAO) and related to the $[Cp(donor)CrR]^+$ species discussed previously[3] and to the metallocenealkyl cations identified as the active species in the case of the group 4 metallocene-based catalysts.[28]

The starting point for our calculations is the cation $[(R_2DC_2H_4C_5H_4)CrPr]^+$ (D = N or P) formed by the insertion of a single ethylene molecule into the initial Cr−Me bond. The preferred routes for the propagation and termination reactions with ethylene *obtained from the calculations* are shown in Figure 3, while the associated relative energies of the intermediates and transition states are listed in Table 5.

In Table 5, a minimum is labeled with a Roman numeral (**I**−**VI**), and in the case of an agostic Cr−H−C structure, this is followed by a Greek letter identifying the carbon atom involved. Transition states are identified by a bracket enclosing the product and the reactant separated by an arrow and followed by the suffix ‡ and the molecular term (high-spin, ^{4}A, or low-spin, ^{2}A).

The numerical results shown in Table 5 can be rationalized by taking into account the electronic structure of the metal atom. The Cr atom in **I** has 15 valence electrons (the agostic H atom is regarded as a dative ligand), and in the high-spin (^{4}A) configuration with three unpaired electrons all nine metal valence orbitals are either singly or doubly occupied. This electronic saturation can be expected to give the system an inherent stability analogous to that observed for an 18-electron species.[3] The high-spin species **Iβ(^{4}A)** has the lowest calculated free energy in the catalytic cycle and is the resting state for the system. Conversion of **I** to the high-spin metal−alkene species **IV(^{4}A)** proceeds with cleavage of an agostic Cr−H bond in a facile, practically thermoneutral process. The subsequent propagation step also proceeds on the high-spin surface; the transition state (TS), **[IV→VIγ]‡(^{4}A)**, has a significantly lower energy than the analogous low-spin (^{2}A) species. In contrast, no TS for termination through β-hydrogen transfer (BHT) could be located on the high-spin surface starting from **IV**, and since coordination of the migrat-

(22) Döhring, A.; Jolly, P. W. Unpublished results.
(23) Thomas, B. J.; Noh, S. K.; Schulte, G. K.; Sendlinger, S. C.; Theopold, K. H. *J. Am. Chem. Soc.* **1991**, *113*, 893.
(24) Rogers, J. S.; Bazan, G. C. *Chem. Commun.* **2000**, 1209.
(25) Margl, P.; Deng, L. Q.; Ziegler, T. *Organometallics* **1999**, *18*, 5701.
(26) Musaev, D. G.; Morokuma, K. *Top. Catal.* **1999**, *7*, 107.
(27) Lohrenz, J. C. W.; Bühl, M.; Weber, M.; Thiel, W. *J. Organomet. Chem.* **1999**, *529*, 11.
(28) Jordan, R. F.; Dasher, W. E.; Echols, S. F. *J. Am. Chem. Soc.* **1986**, *108*, 1718.

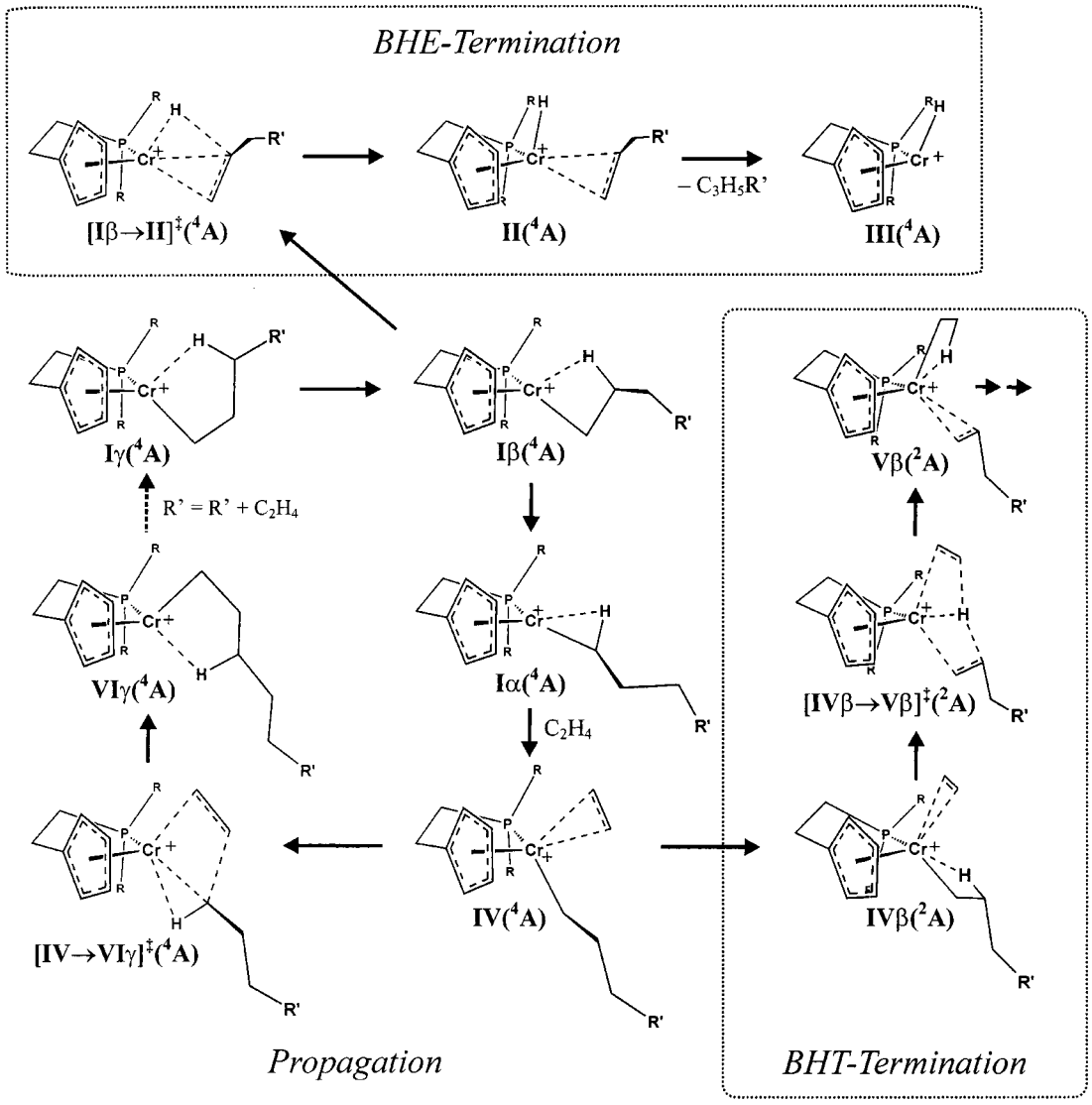

Figure 3. Preferred routes for the propagation and termination reactions of $[(R_2PC_2H_4C_5H_4)Cr-C_3H_6R']^+$ with ethylene from DFT calculations using R′ = H. **Iγ(^{4}A)** and **VIγ(^{4}A)** differ by inversion at the metal center: a further insertion step completes the propagation cycle. Spin inversion in **Vβ(^{2}A)** to form **V(^{4}A)** followed by elimination of the olefinic chain completes the BHT-termination sequence.

ing H atom in the electronically saturated high-spin state is energetically unfavorable, we suggest that *termination through BHT proceeds with spin-pairing* to generate a low-lying, empty d-orbital at the metal, which is then available for hydrogen transfer, i.e., the 17-electron complex **IVβ(^{2}A)** reacts further to give the BHT product **Vβ(^{2}A)**. Alternatively, this empty d-orbital can be generated by decoordination of the donor atom, D. Cr−P bond dissociation in **IV(^{4}A)** of **7a** by a ∼180° rotation around the Cp−C bond of the ethano-bridge produces a 15-electron high-spin complex with a pronounced Cr−H β-agostic interaction that is presumably a starting point for β-hydrogen transfer to the ethylene. However, the free energy of this metal(alkene) species is 19.4 kcal/mol higher than that of **IV(^{4}A)**, which indicates that complexes with a noncoordinated donor do not take part in the BHT termination reaction.

The neutral catalyst precursors are found to have three unpaired electrons (vide supra), in accord with the observation that organometallic complexes of chromium(III) are usually 15-electron systems with a spin quartet ground state,[29] although in some cases it has been possible to stabilize a 17-electron configuration.[30,31] Our calculations indicate that the high-spin state is preferred also for the active catalyst cation, **Iβ(^{4}A)**. For the catalyst derived from **7a**, the adiabatic ^{2}A←^{4}A transition energy in the resting state is more than 10 kcal/mol higher than the free energy of insertion.[32] This suggests that the termination step in the catalytic cycle of **7a** does not involve an excitation of the resting state, **Iβ(^{4}A)**, prior to coordination of the olefin but rather a double spin-inversion on the reaction coordinate between reactants and products: one after ethylene coordination and before β-hydrogen transfer, **IV(^{4}A)/IVβ(^{2}A)**, and a second immediately after β-hydrogen transfer, **Vβ(^{2}A)/**

(29) Cacelli, I.; Keogh, D. W.; Poli, R.; Rizzo, A. *J. Phys. Chem. A* **1997**, *101*, 9801.

(30) Shen, J. K.; Freeman, J. W.; Hallinan, N. C.; Rheingold, A. L.; Arif, A. M.; Ernst, R. D.; Basolo, F. *Organometallics* **1992**, *11*, 3215.

(31) Betz, P.; Döhring, A.; Emrich, R.; Goddard, R.; Jolly, P. W.; Krüger, C.; Romão, C. C.; Schönfelder, K. U.; Tsay, Y. H. *Polyhedron* **1993**, *12*, 2651.

(32) The solution for **Iβ(^{2}A)** is spin-contaminated ($\langle S^2\rangle = 1.75$). Using the correction scheme described in the Computational Details section, ΔH_{298} and ΔG_{298} were calculated to be 26.7 and 27.2 kcal/mol, respectively.

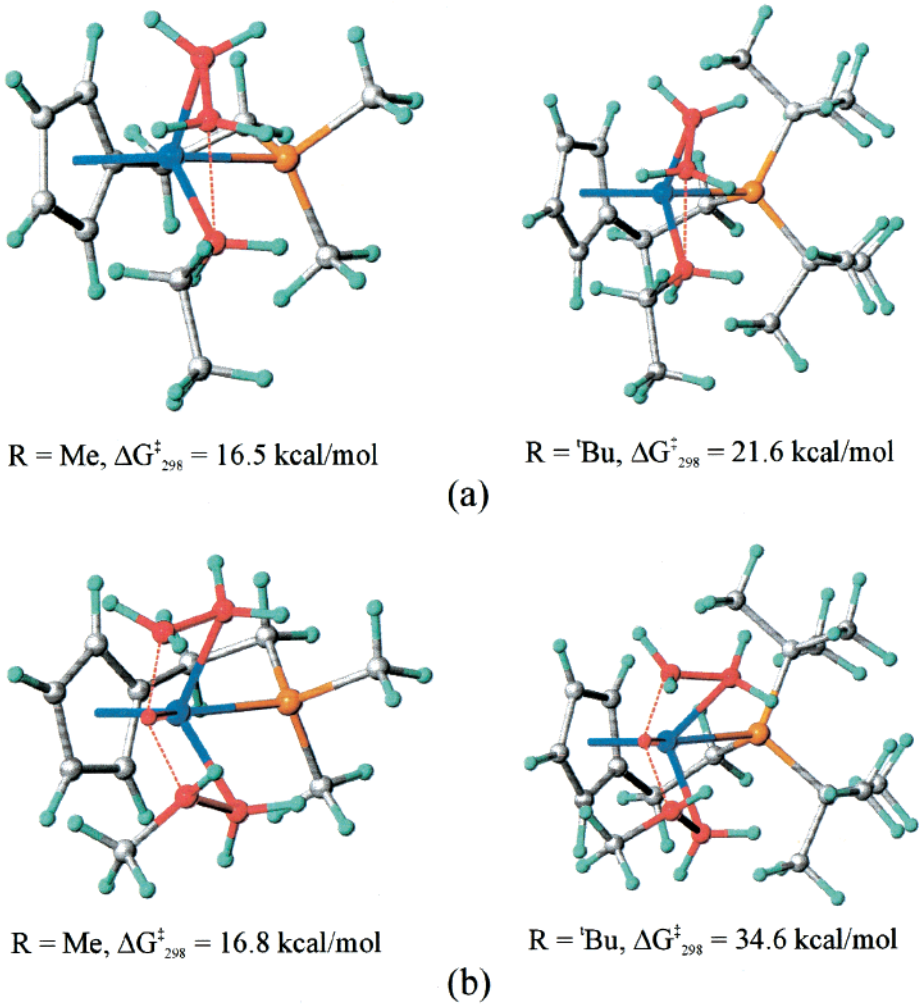

Figure 4. DFT-optimized transition states (TS) for (a) ethylene insertion, **[IV→VIγ]‡(⁴A)** and (b) β-hydrogen transfer (BHT) to ethylene, **[IVβ→Vβ]‡(²A)** for the catalysts derived from **7a** (R = Me) and **7f** (R = ^{t}Bu). The H and C atoms involved in the four- and six-membered metallacycles are shown in red, Cr in dark blue, and P in orange.

V(⁴A). Spin inversion will of course only occur efficiently if the two spin states have similar energies, which is indeed seen to be the case in **7a** for **IV(⁴A)** and **IVβ(²A)** (cf. Table 5). Further work is in progress to identify the minimum energy crossing points as well as to assess their probability of undergoing spin-inversion. It has already been suggested that the principle of two-state reactivity discussed here could well be a "key feature in organometallic chemistry".[33]

An alternative termination process involving complete transfer of the β-hydrogen atom to the metal (β-hydrogen elimination, BHE, see Figure 3) to give a Cr(olefin)H species has been considered but can be neglected as a route to formation of the oligomers obtained with small substituents, R. The rate-determining step in the BHE process is the subsequent elimination of the olefin, **[II→III]‡(⁴A)**, which is associated with an entropic barrier. In the case of **7a** even the separated elimination products (hydride + olefin) have a higher free energy than the transition states for ethylene insertion or BHT. The entropic barrier to elimination of the olefin product (propene) in the ^{t}Bu-substituted system (**7f**) on the other hand is lower than that of the BHT step although still significantly higher than that of chain propagation.

As can be seen from Table 5, the activation free energy ($\Delta G^{\ddagger}_{298}$) of insertion, **[IV→VI$\gamma$]‡(⁴A)**, and termination through BHT, **[IVβ→Vβ]‡(²A)**, are calculated to be almost identical (±1 kcal/mol) for the phosphino-substituted system with R = Me, whereas in the case of R = ^{t}Bu insertion is favored over termination by more than 10 kcal/mol for BHT and about 4 kcal/mol for BHE. In other words, the rates of insertion and termination are predicted to be of the same order for the catalyst derived from **7a** (R = Me), and as a consequence the reaction will be terminated after a few insertion steps and the product will be predominantly short-chain olefins. In contrast, in the case of the catalyst derived from **7f** (R = ^{t}Bu) the rate of insertion will be several orders of magnitude larger than the rate of termination and multiple insertion can be expected before termination occurs and the product will be polymeric. Distinct differences in barrier heights (~9−11 kcal/mol) in favor of insertion compared to BHT and BHE termination are also seen for the dimethylamino-substituted system, which has already been shown to produce mainly polyethylene.[2]

Figure 4 shows a pictorial representation of the transition states for ethylene insertion (Figure 4a) and

(33) Schröder, D.; Shaik, S.; Schwarz, H. *Acc. Chem. Res.* **2000**, *33*, 139.

chain termination through BHT (Figure 4b) for the catalysts derived from **7a** and **7f**. As can be seen, the six-membered metallacycle involved in the termination sequence occupies more space than the four-membered metallacycle formed during chain propagation. Both metallacycles adopt a position more or less perpendicular to a plane described by the center of the Cp ring and the Cr and P atoms, and whereas a P-bonded methyl group has only a small steric influence, the introduction of a *tert*-butyl group results in the effective blocking of the axial positions above and below this plane by methyl groups. The resulting destabilization of the transition states is particularly marked in the case of the six-membered metallacycle, and as a result chain termination through BHT is suppressed.

A similar strategy has been discussed for the catalysts derived from the (bisimine)Ni(II) compounds (**21**) developed by Brookhart et al.[34,35] In our case, the distorted tetrahedral configuration around the P atom will ensure that the P−R bonds are directed out of the equatorial Cp−Cr−P, plane causing the substituents to block the axial positions and forcing the two olefin moieties closer together to give a more compact TS.

The N atom is smaller than the P atom, and hence the Cr−D and D−R distances will be shorter for the amino-substituted systems than for the phosphino-substituted systems, while the associated Tolman cone angle[13] will be more acute in the former case. As a result, the BHT transition state will be more compact for the Me_2N-substituted species than for the Me_2P-substituted species, the barrier to BHT will be much higher than for insertion, and as a result multiple insertion with polymer formation occurs.[2] Conversely, increasing the size of the donor atom by replacing phosphorus by arsenic would be expected to lead to an increase in oligomer formation, and this is indeed observed for the system $(Cy_2AsC_2H_4C_5H_4)CrCl_2$−MAO.[1]

The results presented above indicate that both the observed and calculated trends in catalytic activity have a steric origin: bulky substituents destabilize the structures **IV**−**VI** (and hence the TS of insertion) to a greater extent than the monomer-free resting state **I**β**(4A)**, and hence the activity is expected to decrease upon increasing the size of the substituents on the P atom. Interestingly, this is in contrast to the trend reported for the N-aryl-substituted (bisimine)Ni catalysts, for which the metal−alkene complex is suggested to constitute the resting state.[14,34−36] The negative effect of steric crowding upon the activity is also consistent with the observation that the P-containing catalysts are apparently more active than the related N-containing systems: the calculated barrier to propagation for **7a** ($\Delta G^{\ddagger}_{298}$ = 16.5 kcal/mol) is found to be slightly lower than that for the dimethylamino species ($\Delta G^{\ddagger}_{298}$ = 17.1 kcal/mol).

Experimental Section

All experiments and manipulations were carried out under argon. The compounds have been characterized by a combination of elemental analyses and spectroscopic methods. The chromium complexes are paramagnetic, and the structural characterization is based largely on crystal structural analyses of selected compounds.

The $R_2PC_2H_4C_5H_4Li$ (**1**)[10] and $R_2PC_2H_4$IndenylLi (**2**)[37] derivatives have been prepared by reacting the appropriate lithium phosphide with either spiro[2.4]hepta-4,6-diene[8] or spiro[cyclopropane-1,1′-indene].[9] $R_2PC_3H_6C_5H_4Li$ (**3**)[10] and $Cy_2PC_3H_6$IndenylLi (**4**) were prepared by reacting $R_2PC_3H_6Cl$ with either NaCp/BuLi or IndenylLi, $Ph_2PC_3H_6C_5Me_4Li$ (**5**)[11] by reacting $LiPPh_2$ with $TosOC_3H_6C_5Me_4H$, and $Cy_2AsC_2H_4C_5H_4Li$ (**6**) by reacting $LiAsCy_2$ with spiro[2.4]hepta-4,6-diene in a manner similar to that described earlier.[12] The preparation of representative examples that have not previously been adequately described are reported below.

$Me_2PC_2H_4C_5H_5$ (1a). $LiPMe_2$ was prepared by reacting $PhPMe_2$ (4.00 g, 29 mmol) with Li-sand (0.66 g, 94.25 mmol) in THF (60 mL). The resulting brown solution was cooled to 0 °C and stirred for 12 h. The reaction mixture was filtered through glass wool (to remove the unreacted lithium) and ^{t}-BuCl (1.59 g, 17.4 mmol) added to the red-brown solution to destroy the PhLi generated. The reaction mixture was then added to spiro[2.4]hepta-4,6-diene (1.60 g, 17.4 mmol) in THF (50 mL) and refluxed for 2 h. The reaction mixture was evaporated to dryness in an oil-pump vacuum, and the orange residue washed several times with pentane. The product was suspended in pentane (50 mL) and hydrolyzed with water (50 mL). The organic phase was washed (3 × 50 mL) and dried with sodium sulfate, and the product isolated by distillation (21−25 °C, 0.02 mbar) and shown by NMR to consist of a mixture of two isomers. Yield: 1.47 g (33%). IR (KBr): ν 2953, 2922, 2893, 1430, 937, 897, 707. MS (EI): *m/e* 154 (M^+), 139, 126, 111. ^{1}H NMR ($CDCl_3$): δ 6.46−6.39/6.26−6.23/6.18−6.17/6.04−6.01 (:CH), 2.93/2.88 (CH), 2.50/1.60 (C_2H_4), 1.02 (Me). ^{13}C NMR ($CDCl_3$): δ 135.22/133.14/131.38/127.08/126.45 (C_5H_5), 43.32/41.37 (C_5H_5), 32.09/31.22/26.93/26.12 (C_2H_4), 13.88 (Me). ^{31}P NMR ($CDCl_3$): δ −50.11.

$Et_2PC_2H_4C_5H_4Li$ (1b). $LiPEt_2$ (1.32 g, 13.75 mmol), prepared by treating Et_2PH with BuLi in pentane, was dissolved in THF (50 mL) and treated with spiro[2.4]hepta-4,6-diene (1.27 g, 13.75 mmol) and refluxed for 1 h. The resulting yellow-green solution was evaporated to dryness and the residue washed with pentane to give the compound as a colorless powder having 74% (NMR) purity. Yield: 2.36 g (91%). MS (EI, −10 °C): *m/e* 182 (M^+ + H/−Li), 167, 154, 139, 125. ^{1}H NMR (THF-d_8): δ 5.54 (C_5H_4), 2.59/1.60 (C_2H_4), 1.36/1.06 (Et). ^{13}C NMR (THF-d_8): δ 31.19/27.03 (C_2H_4), 19.42/9.91 (Et). ^{31}P NMR (THF-d_8): δ −23.87.

$Cy_2PC_2H_4C_5H_4Li$ (1c) was prepared similarly. Yield: 91%. IR (KBr): ν 2923, 2850, 1446. MS (EI): *m/e* 290 (M^+ + H/−Li), 208, 126. ^{1}H NMR (THF-d_8): δ 5.6 (C_5H_4), 2.65 (C_2H_4), 1.9−1.6/1.5−1.1 (Cy/C_2H_4). ^{13}C NMR (THF-d_8): δ 120.87/102.80/102.49 (C_5H_4), 34.14/31.38/30.09/29.44/29.07/28.24/27.44/25.76 (Cy/C_2H4). ^{31}P NMR (THF-d_8): δ −7.99.

1-$Cy_2PC_2H_4$Indene (2c). Spiro[cyclopropane-1,1′-indene] (3.55 g, 25 mmol) was added at room temperature to $LiPCy_2$ (5.10 g, 25 mmol) in THF (100 mL) and refluxed for 1 h. The reaction mixture was evaporated to dryness under oil-pump vacuum and the resulting red oil treated with pentane (100 mL) and hydrolyzed with water (200 mL). The organic phase was washed (3 × 50 mL), dried with sodium sulfate, and distilled to give the compound in 85% (NMR) purity as an oil (bp 192 °C, 0.02 mbar). Yield: 2.21 g (26%). IR (KBr): ν 2923, 2849, 1446, 769, 718. MS (EI, 75 °C): *m/e* 340 (M^+), 258, 176. ^{1}H NMR ($CDCl_3$): δ 7.38/7.28/7.22/7.13/6.18 (indene), 3.26 (indenylH), 2.67−2.55/1.90−1.45/1.30−1.05 (Cy/C_2H_4). ^{13}C NMR ($CDCl_3$): δ 145.32/145.07/144.39 (indene), 127.20/125.77/124.30/123.51/118.61 (indene), 36.6/32.4/29.57/28.27/26.57/26.45/26.25/25.69/18.88 (Cy/C_2H_4). ^{31}P NMR ($CDCl_3$): δ −1.81.

(34) Johnson, L. K.; Killian, C. M.; Brookhart, M. *J. Am. Chem. Soc.* **1995**, *117*, 6414.
(35) Deng, L. Q.; Woo, T. K.; Cavallo, L.; Margl, P. M.; Ziegler, T. *J. Am. Chem. Soc.* **1997**, *119*, 6177.
(36) Froese, R. D. J.; Musaev, D. G.; Morokuma, K. *J. Am. Chem. Soc.* **1998**, *120*, 1581.
(37) Kataoka, Y.; Saito, Y.; Shibahara, A.; Tani, K. *Chem. Lett.* **1997**, 621.

$Cy_2PC_3H_6C_5H_4Li$ (3a). 3-Chlor-1-(dicyclohexylphosphano)-propane (11.6 g, 42.3 mmol) and NaCp (14.9 g, 126.9 mmol, 75% pure) were dissolved in THF (200 mL) and heated under reflux for 14 h. The reaction mixture was evaporated to dryness under oil-pump vacuum and the residue suspended in diethyl ether (200 mL) and hydrolyzed with water. The organic phase was washed with water (3 × 200 mL), dried with sodium sulfate, and evaporated to dryness. The residue was taken up in pentane (100 mL) and treated with excess BuLi (42.3 mmol from a 1.653 M solution in hexane) at 0 °C. The compound was deposited as a white precipitate, which was isolated and washed with a little pentane. Yield: 6.72 g having 85% (NMR) purity (51%). IR (KBr): ν 2923, 2850, 1447, 754. MS (EI, 210 °C): *m/e* 310 (M^+), 303, 227, 204, 130. ^{1}H NMR (THF-d_8): δ 5.57−5.53(C_5H_4), 2.56 (CH_2), 1.9−1.1 (Cy/CH_2). ^{13}C NMR (THF-d_8): δ 119.40/102.33/1.1.61 (C_5H_4), 34.04/32.86/32.24/30.82/29.46/27.80/27.68/26.99/22.0 (C_3H_6/Cy). ^{31}P NMR (THF-d_8): δ −4.63.

1-$Cy_2PC_3H_6$Indene (4). A solution of indenyl-Li (6 g, 49.2 mmol) in THF (200 mL) was added at 0 °C to 3-chloropropyl-dicyclohexylphosphane (4.50 g, 16.4 mmol) dissolved in THF (50 mL). The reaction mixture was then hydrolyzed with water (300 mL), and the organic phase was separated and washed with water (3 × 50 mL) and dried over sodium sulfate. The excess indene was distilled off under oil-pump vacuum. The brown residue was dissolved in pentane (100 mL) and treated with BuLi (16.4 mmol in hexane). A red oil was formed, which was isolated by decantation. Yield: 0.56 g (10%). ^{1}H NMR ($CDCl_3$): δ 7.5−7.16.2 (indene), 3.2, 2.6, 2.0−1.0 (C_2H_4/Cy). ^{13}C NMR ($CDCl_3$): δ 145.11/144.10/143.85 (indene), 127.51/125.69/124.11/123.33/118.65 (indene), 37.36 (indene), 33.06/30.99/29.13/28.75/27.15/26.99/26.94/21.10/20.78 (C_2H_4/Cy). ^{31}P NMR ($CDCl_3$): δ −4.37.

$Cy_2AsC_2H_4C_5H_4Li$ (6). A solution of spiro[2.4]hepta-4,6-diene (6.12 g, 66.5 mmol) and $LiAsCy_2$ (13.57 g, 66.5 mmol), prepared by reacting Cy_2AsCl with $LiAlH_4$ in diethyl ether, was refluxed in THF (250 mL) for 5 h. The resulting brown suspension was evaporated to dryness in an oil-pump vacuum and the residue washed with pentane to give the compound as a white powder. Yield: 16.61 g (73%). Anal. Calcd for $C_{19}H_{30}$AsLi: C, 67.1; H, 8,9; As, 22.0; Li, 2.0. Found: C, 66.9; H, 8.8; As, 22.2; Li, 2.1. IR (KBr): ν 2962, 2921, 2849, 1446. MS (EI, 50 °C): *m/e* 334 (M^+ + H/−Li), 252, 169. ^{1}H NMR (THF-d_8): δ 5.42 (C_5H_4), 2.58−2.52 (C_2H_4), 1.63−1.48/1.25−1.15 (Cy). ^{13}C NMR (THF-d_8): δ 124.87/105.56/105.42 (C_5H_4), 37.56/35.40/34.30/32.93/31.85/30.71 (Cy).

(η^1: η^5-$Et_2PC_2H_4C_5H_4$)$CrCl_2$ (7b) was prepared by adding a solution of $C_5H_4C_2H_4PEt_2Li$ (2.35 g, 12.5 mmol) in THF (40 mL) at −78 °C to a solution of $Cr(THF)_3Cl_3$ (4.68 g, 12.5 mmol) in THF (50 mL). The resulting blue solution was allowed to reach room temperature overnight and then evaporated to dryness. The residue was washed with pentane and extracted with boiling toluene. Cooling the extract gave the compound as blue needles. Yield: 1.54 g (40%). Anal.: see Table 1. IR (KBr): ν 3076, 2883, 1382, 1048, 810, 765. MS (EI, 135 °C): *m/e* 303 (M^+ − H), 268, 231, 203.

The following compounds were prepared similarly to that described above by reacting $Cr(THF)_3Cl_3$ with the appropriate Li-salt, $C_5H_4C_2H_4PR_2Li$, in THF. The elemental analyses are listed in Table 1.

(η^1:η^5-$Me_2PC_2H_4C_5H_4$)$CrCl_2$ (7a): blue needles; IR (KBr) ν 3082, 1479, 1417, 962, 914, 818; MS (EI, 140 °C) *m/e* 275 (M^+ − H), 260, 240, 203, 178.

(η^1:η^5-$Pr_2PC_2H_4C_5H_4$)CrCl2 (7c): blue; IR (KBr) ν 2959, 2931, 1453, 1080, 815; MS (EI, 120 °C) *m/e* 331 (M^+), 209.

(η^1:η^5-$^i Pr_2PC_2H_4C_5H_4$)$CrCl_2$ (7d): blue needles; IR (KBr) ν 2977, 2946, 2917, 2871, 1454, 1382, 1365, 1248, 1035, 819; MS (EI, 125 °C) *m/e* 331 (M^+ − H), 296, 259, 217.

(η^1:η^5-$^i Bu_2PC_2H_4C_5H_4$)$CrCl_2$ (7e): blue IR (KBr) ν 3077, 2927, 1405, 1383, 1258, 1162, 1066, 829; MS (EI, 105 °C) *m/e* 359 (M^+), 237.

(η^1:η^5-$^t Bu_2PC_2H_4C_5H_4$)$CrCl_2$ (7f): blue needles; IR (KBr) ν 3000, 2986, 2961, 2868, 1473, 1371, 1361, 1174, 1022, 823; MS (EI, 155 °C) *m/e* 359 (M^+ − H), 324, 267.

(η^1:η^5-$Neopentyl_2PC_2H4C_5H_4$)$CrCl_2$ (7g): blue powder; IR (KBr) ν 3094, 2947, 2904, 2864, 1475, 1387, 1234,1031, 818; MS (EI, 145 °C) *m/e* 387 (M^+).

(η^1:η^5-$Hexyl_2PC_2H_4C_5H_4$)$CrCl_2$ (7h): dark blue; IR (KBr) ν 3067, 2955, 2858, 1451, 811; MS (EI, 125 °C) *m/e* 415 (M^+).

(η^1:η^5-$Cy_2PC_2H_4C_5H_4$)$CrCl_2$ (7i): IR (KBr) ν 2927, 2856, 1444, 811; MS (EI) *m/e* 411 (M^+ − H), 376, 339; magn. suscept. (SQUID) μ_{eff}/μ_B 3.5 $_B$. Crystal structure determination: see Figure 1 and Table 3.

(η^1:η^5-$Ph_2PC_2H_4C_5H_4$)$CrCl_2$·toluene (7j′): IR (KBr) ν 1433, 1384, 828, 738, 693; MS (EI, 100 °C) *m/e* 399 (M^+ − C_7H_8/H), 364, 327. Crystal structure determination: see Figure 1 and Table 3.

The toluene molecule is eliminated when the compound is heated under high vacuum to 100 °C for 6 h to give **(η^1:η^5-$Ph_2PC_2H_4C_5H_4$)$CrCl_2$ (7j)**.

(η^1:η^5-o-$Tolyl_2PC_2H_4C_5H_4$)$CrCl_2$ (7k): IR (KBr) ν 1476, 1449, 1436, 1412, 827, 754; MS (EI, 205 °C) *m/e* 427 (M^+ − H), 392, 355.

(η^1: η^5-1-$Naphthyl_2PC_2H_4C_5H_4$)$CrCl_2$·Me_2CO (7l′). In contrast to the other examples, this compound was extracted with acetone. IR (KBr): ν 1716, 1636, 1506, 1413, 1359, 1220, 797, 773. MS (EI, 195 °C): *m/e* 499 (M^+ − H), 464, 428.

Thermolysis at 180 °C under high vacuum for 72 h leads to the formation of the solvent-free compound **(η^1:η^5-1-Naphthyl$_2$PC$_2$H$_4$C$_5$H$_4$)CrCl$_2$ (7l):** IR (KBr) ν 3110, 1506, 1414, 1359, 1213, 1091, 843, 827, 800, 773; MS (EI) *m/e* 499 (M^+ − H), 464, 428.

(η^1:η^5-$Et_2PC_2H_4$Indenyl)$CrCl_2$ (8a) was prepared by adding 1-indenyl$C_2H_4PEt_2Li$ (27 mL of a 0.112 mmol/mL solution in THF, 3.02 mmol) to a solution of $Cr(THF)_3Cl_3$ (1.25 g, 3.32 mmol) in THF (50 mL) at −78 °C. The resulting green reaction mixture was allowed to warm to room temperature over 16 h and then evaporated to dryness to give a green oil, which was extracted with toluene/CH_2Cl_2. The extract was filtered and evaporated to give the compound as a green solid. Yield: 0.65 g (61%). Anal.: see Table 1. IR (KBr): ν 3065, 2964, 2935, 1609, 1526, 1455, 1412, 1031, 751. MS: dec.

The following compounds were prepared similarly to that described above by reacting $Cr(THF)_3Cl_3$ with the Li-salt of the appropriate 1-indenyl derivative in THF and extracted with toluene.

(η^1:η^5-$^i Bu_2PC_2H_4$Indenyl)$CrCl_2$ (8b): green. IR (KBr) ν 2957, 2869, 1464, 1402, 1366, 1070, 806, 752; MS (EI; 145 °C) 409 (M^+).

(η^1:η^5-$Cy_2PC_2H_4$Indenyl)$CrCl_2$ (8c): green needles; IR (KBr) ν 3080, 2926, 2850, 1446, 754, 742; MS (EI, 185 °C) *m/e* 461 (M^+ − H), 425, 389.

(η^1:η^5-$Cy_2PC_3H_6C_5H_4$)$CrCl_2$ (9a) was prepared as a dark blue solid by adding a solution of $LiCy_2PC_3H_6C_5H_4$ (6.67 g, 22 mmol) in THF (50 mL) to $Cr(THF)_3Cl_3$ (8.24 g, 22 mmol) dissolved in THF (50 mL) at room temperature. The reaction mixture was evaporated to dryness and the residue washed with pentane and extracted with toluene. The compound was precipitated at −30 °C by adding pentane to the extract. Yield: 2.87 g. (31%). Anal.: see Table 1. IR (KBr): ν 2928, 2852, 1445, 847, 814, 785. MS (EI, 175 °C): *m/e* 425 (M^+ − H), 390, 353. Crystal structure determination: see Figure 2 and Table 3.

(η^1:η^5-$Ph_2PC_3H_6C_5H_4$)$CrCl_2$ (9b) was prepared similarly as blue needles. Anal.: see Table 1. IR (KBr): ν 2918, 2849, 1481, 1435, 1404, 741, 698. MS (EI, 170 °C): *m/e* 413 (M^+ − H), 378, 342.

(η^1:η^5-$Cy_2PC_3H_6$Indenyl)$CrCl_2$ (10) was prepared by adding 1-indenyl$C_3H_6PCy_2Li$ (1.6 mmol) in THF (30 mL) to a solution of $Cr(THF)_3Cl_3$ (0.82 g, 2.2 mmol) in THF (50 mL) at room temperature. The dark green reaction mixture was evaporated to dryness and the residue washed with pentane

(3 × 30 mL) and then extracted with toluene. The compound was precipitated as green needles by adding pentane. Yield: 0.11 g (9%). Anal.: see Table 1. IR (KBr): ν 2924, 2849, 1448, 812, 805, 758. MS (EI, 160 °C): *m/e* 475 ($M^+ - H$), 440, 403.

(η^1:η^5-$Ph_2PC_3H_6C_5Me_4$)$CrCl_2$ (11). A solution of $LiPh_2PC_3H_6C_5Me_4$ (prepared from $Ph_2PC_3H_6C_5Me_4H$ (23.25 g, 66.8 mmol) and ^{t}BuLi (66.8 mmol) in THF/hexane at 0 °C) was added to $Cr(THF)_3Cl_3$ (21.81 g, 66.8 mmol) in THF (100 mL) at room temperature. The green reaction mixture was evaporated to dryness under oil-pump vacuum and the residue dissolved in toluene. The toluene solution was filtered through Celite (to remove a green impurity) and the resulting blue solution evaporated to dryness. The residue was washed with pentane and recrystallized from boiling toluene. Yield: 8.5 g (27%). Anal.: see Table 1. IR (KBr): ν 2954, 2919, 2866, 1484, 1435, 1378, 1096, 741, 695, 518. MS (EI, 140 °C): *m/e* 469 ($M^+ - H$), 434, 398. Crystal structure determination: see Figure 2 and Table 3.

(η^1:η^5-$Cy_2PC_2H_4C_5H_4$)Cr(Et)Br (12) was prepared by reacting a solution of ($Cy_2PC_2H_4C_5H_4$)$CrCl_2$ (**7i**) (0.82 g, 2 mmol) in THF (20 mL) with 2 equiv of EtMgBr (1.46 M solution in diethyl ether) at −78 °C. The reaction mixture was allowed to reach room temperature overnight and evaporated to dryness. The residue was washed with pentane and extracted with toluene. Filtration and cooling the extract to −78 °C gave the compound as a brown powder. Yield: 0.22 g (24%). Anal.: see Table 2. IR (KBr): ν 2925, 2851, 1442, 804. MS (EI, 120 °C): *m/e* 422 ($M^+ + H/-Et$), 341, 257, 177.

(η^1:η^5-$Cy_2PC_2H_4$Indenyl)Cr(Me)Cl (13) was prepared as a violet powder by adding 2 equiv of MeMgCl (2.73 M in THF) to ($Cy_2PC_2H_4$Indenyl)$CrCl_2$ (**8c**) (0.26 g, 0.6 mmol) in THF (10 mL) at −78 °C. The resulting violet solution was warmed to room temperature and evaporated to dryness, and the residue was washed with pentane and taken up in toluene. This procedure was repeated twice to remove traces of unreacted MeMgCl and the compound precipitated by adding pentane to a toluene solution. Yield: 0.06 g (17%). Anal.: see Table 2. IR (KBr): ν 2924, 2849, 1446, 747. MS (EI, 185 °C): *m/e* 441 (M^+), 426.

(η^1:η^5-$Et_2PC_2H_4C_5H_4$)$CrMe_2$ (14) was prepared by adding a solution of MeMgCl (10 equiv of a 2.73 M solution in THF) to ($Et_2PC_2H_4C_5H_4$)$CrCl_2$ (**7b**) (0.59 g, 1.9 mmol) in THF (20 mL) at −30 °C. Warming the reaction mixture to room temperature was accompanied by a color change from blue, to violet, to blue-green. The reaction mixture was evaporated to dryness and the residue extracted with pentane. This procedure was repeated several times until the extract was homogeneous. The compound was isolated as blue-violet needles by cooling the final pentane extract to −80 °C. Yield: 0.11 g (22%). Anal.: see Table 2. IR (KBr): ν 2935, 2780, 1456, 1418, 1379, 1029, 804. MS (EI, 75 °C): *m/e* 264 ($M^+ + H$), 263, 248, 233, 219, 205, 191.

The following compounds were prepared similarly to that described above by reacting the appropriate ($R_2PC_2H_4C_5H_4$)$CrCl_2$ compound with a Grignard reagent or MeLi (**15a**) in THF/diethyl ether. The analytical data are listed in Table 2. In addition, **(η^1:η^5-$Cy_2PC_2H_4C_5H_4$)$CrPr_2$** was isolated as a green solid at −30 °C (yield: 48.3%) but proved too unstable to analyze.

(η^1:η^5-$Cy_2PC_2H_4C_5H_4$)$CrMe_2$ (15a): green-black needles; IR (KBr) ν 2924,2852, 2780, 1448, 784; MS (EI, 95 °C) *m/e* 371 (M^+), 356, 338, 256, 177; magn. suscept. (SQUID) μ_{exp}/μ_B 3.5 $_B$. Crystal structure determination: see Figure 1 and Table 3.

(η^1:η^5-$Cy_2PC_2H_4C_5H_4$)Cr^tBu_2 (15b): dark green needles; IR (KBr) ν 2924, 2850, 2795, 2735, 1449, 1411, 1368, 1349, 793; MS (EI, 100 °C) *m/e* 455 (M^+), 398, 341, 338, 258.

(η^1:η^5-$Ph_2PC_2H_4C_5H_4$)$CrPr_2$ (16a): dark green, decomposes at room temperature; IR (KBr) ν 2940, 2854, 1435, 794, 740, 694; MS (EI, 95 °C) *m/e* 415 (M^+), 372, 329.

(η^1:η^5-$Ph_2PC_2H_4C_5H_4$)Cr^tBu_2 (16b): green, decomposes at room temperature; IR (KBr) ν 2937, 2852, 2824, 1482, 1367, 1351, 1184, 1098, 1027, 795, 736, 691; MS (EI, 80 °C) dec.

(η^1:η^5-$Ph_2PC_2H_4C_5H_4$)$CrCy_2$ (16c): green, decomposes at room temperature; IR (KBr) ν 2901, 2825, 2769, 1481, 1433, 795, 750, 693; MS (EI, 100 °C) dec.

(η^1:η^5-$Cy_2PC_3H_6C_5H_4$)$CrMe_2$ (17) was prepared as blue-violet needles by adding 2 equiv of MeMgCl (2.73 M solution in THF) to a solution of ($Cy_2PC_3H_6C_5H_4$)$CrCl_2$ (**9a**) (0.29 g, 0.7 mmol) in THF (20 mL) at room temperature. The reaction mixture was evaporated to dryness and the compound extracted with pentane and precipitated by cooling to −30 °C. Yield: 0.11 g (45%). Anal.: see Table 2. IR (KBr): ν 2921, 2853, 2779, 1442, 792, 781. MS (EI, 120 °C): *m/e* 385 (M^+), 370, 352, 270.

(η^1:η^5-$Ph_2PC_3H_6C_5Me_4$)$CrMe_2$ (18) was prepared by reacting the compound described above (0.94 g, 2 mmol) with MeLi (4.2 mmol of a 1.6 M solution in THF) at −70 °C. The reaction mixture was warmed to room temperature and at −30 °C changed color from blue to violet. The mixture was evaporated to dryness and the residue extracted with pentane. Cooling the pentane solution to −30 °C gave the compound as small black needles. Yield: 0.02 g (2%). Anal: see Table 2. IR (KBr): ν 2901, 2853, 1481, 1378, 739, 694. MS (EI, 110 °C): *m/e* 429 (M^+), 414, 398.

(η^1:η^5-$Cy_2AsC_2H_4C_5H_4$)$CrCl_2$ (19) was prepared by adding $LiC_5H_4C_2H_4AsCy_2$ (6.61 g, 48.8 mmol) dissolved in THF (200 mL) to a solution of $Cr(THF)_3Cl_3$ (18.28 g, 48.8 mmol) in THF (200 mL) at room temperature. The resulting dark blue solution was evaporated to dryness under high vacuum and the residue extracted with toluene. The compound was recrystallized from boiling toluene as blue platelets. Yield: 15.9 g (72%). Anal. Calcd for $C_{19}H_{30}AsCl_2Cr$: C, 50.0; H, 6.6; As, 16.4; Cl, 15.5; Cr, 11.4. Found: C, 50.1; H, 6.6; As, 16.4; Cl, 15.5; Cr, 11.5. IR (KBr): ν 3090, 2926, 2854, 1443, 813. MS (EI, 145 °C): *m/e* 455 ($M^+ - H$), 420, 372, 337. Crystal structure determination: see Figure 1 and Table 3.

(η^1:η^5-$Cy_2AsC_2H_4C_5H_4$)$CrMe_2$ (20) was prepared as small green-black needles by reacting **19** (2.59 g, 5.7 mmol) in THF (40 mL) with 2 equiv of MeMgCl (2.73 M solution in THF) at −30 °C. The resulting green solution was allowed to warm to room temperature and evaporated to dryness under high vacuum. The compound was obtained by cooling a pentane extract of the residue to −30 °C. Yield: 0.92 g (39%). Anal. Calcd for $C_{21}H_{36}AsCr$: C, 60.7; H, 8.7; As, 18.0; Cr, 12.5. Found: C, 60.6; H, 8.7; As, 18.1; Cr, 12.6. IR (KBr): ν 2923, 2885, 2780, 1446, 1339, 1264, 1179, 994, 785. MS (EI, 100 °C): *m/e* 415 (M^+), 400, 382.

Catalytic Reactions. The oligomerization reactions were carried out in a thermostated glass autoclave (Büchi, BEP 280), and the procedure was similar to that described earlier.[2] The reaction was terminated by simultaneously closing the ethylene valve and injecting propanol (5 mL) into the reactor.

Crystal Structure Determinations. The crystal structure analyses of compounds **7i**, **7j′**, **15a**, **19**, **9a**, and **11** were carried out using a CAD-4 single-crystal diffractometer (Enraf-Nonius). Crystallographic data and details of the refinement are listed in Table 6. Final coordinates and equivalent isotropic thermal parameters are included in the Supporting Information.

Computational Details. The study used gradient-corrected density functional theory (DFT) with the gradient corrections included self-consistently during both geometry optimization and energy evaluation. We have employed the local exchange−correlation potential developed by Vosko et al.[38] augmented with Becke's[39] nonlocal exchange corrections and Perdew and Wang's[40] nonlocal correlation corrections. The

(38) Vosko, S. H.; Wilk, L.; Nusair, M. *Can. J. Phys.* **1980**, *58*, 1200.
(39) Becke, A. D. *Phys. Rev. A* **1988**, *38*, 3098.
(40) Perdew, J. P.; Wang, Y. *Phys. Rev. B* **1992**, *45*, 13244.

Table 6. Crystallographic Data

	7i	7j′	15a	19	9a	11
formula	$C_{19}H_{30}Cl_2CrP$	$C_{26}H_{26}Cl_2CrP$	$C_{21}H_{36}CrP$	$C_{19}H_{30}Cl_2CrAs$	$C_{20}H_{32}Cl_2CrP$	$C_{24}H_{28}Cl_2CrP$
mol wt	412.30	492.34	371.47	456.25	426.33	470.33
cryst size, mm	0.11 × 0.53 × 0.60	0.14 × 0.32 × 0.63	0.11 × 0.18 × 0.35	0.07 × 0.19 × 0.34	0.46 × 0.32 × 0.18	1.16 × 0.60 × 0.77
V (Å^3)	2013.0(7)	1195.8(3)	2074.0(4)	2010.0(3)	2073.7(5)	9251.6(13)
ρ_{calcd} (g/cm^3)	1.360	1.367	1.190	1.508	1.366	1.351
T_{meas} (°C)	20	20	20	20	20	20
λ(Mo Kα) (Å)	0.71069	0.71069	0.71069	0.71069	0.71069	0.71069
Z	4	2	4	4	4	16
μ_{abs} (mm^{-1})	0.911	0.780	0.628	2.466	0.887	0.802
no. rflns msd	4591	4854	4211	7635	3627	9379
no. rflns obsd	3626	3209	2649	6358	2228	5206
no. variables	328	375	208	328	217	505
space group (No.)	$P2_1/n$ (14)	P1 (2)	$P2_1/n$ (14)	$P2_1/n$ (14)	$P2_1/n$ (14)	*Pbca* (61)
a (Å)	8.396(2)	9.2684(10)	8.5482(9)	8.4350(10)	13.693(2)	16.6206(11)
b (Å)	20.064(3)	9.7942(11)	19.671(3)	20.1530(10)	7.5311(9)	29.5156(15)
c (Å)	12.398(3)	14.477(3)	12.7262(11)	12.3500(3)	20.151(3)	18.859(2)
α (deg)	90	98.722(11)	90	90	90	90
β (deg)	105.44(2)	96.066(11)	104.263(8)	106.780(10)	93.662(12)	90
γ (deg)	90	110.833(8)	90	90	90	90
R	0.0434	0.0361	0.0466	0.0624	0.0464	0.0469
R_w	0.1197	0.1054	0.1277	0.1681	0.1249	0.1155
rsd electron density (e Å^{-3})	0.556	0.319	0.457	1.869	0.775	0.377

resulting BPW91 functional was used in the spin-unrestricted formulation implemented in the Gaussian 98 set of programs,[41] and stability tests of the resulting solutions were performed. Extensive studies[42,43] show that the BPW91 functional is capable of providing accurate energy profiles for the monomer insertion step during metal-catalyzed olefin polymerization.

During the geometry optimizations, a contracted [10s,8p,-3d] basis was applied for Cr.[42] P, N, C, and H were described by standard Dunning−Hay[44] valence double-ζ basis sets, with a scale factor of 1.2 (1.15) applied for the inner (outer) exponents of H (exception: ^{t}Bu-methyl groups represented by STO-3G sets[45]). Polarization functions were added to C atoms ($\alpha_d = 0.75$) being part of the ethylene or the polymer chain as well as to P and N ($\alpha_d = 0.60$ and 0.80, respectively). The Gaussian 98[41] defaults were applied for integration grid and convergence criteria. Each stationary point was characterized through analytical calculation of the second derivative matrix. Zero-point and thermal corrections to the energies were computed from the harmonic frequencies using standard procedures. The barrier to elimination of the olefinic chain from the chromium hydride, **II(⁴A)**, was found to be entropic in nature, and estimates thereof were obtained by stepwise geometry optimization and vibrational analysis with constrained Cr−C(propene) distances to locate the maximum on the free energy curve of propene decoordination.

All energies reported in the current work are based on single-point energy calculations using basis sets that were improved compared to those of the geometry optimizations: C and H atoms forming part of the ethylene or the polymer chain were described by augmented Dunning triple-ζ sets denoted TZD2P[43] to account for known basis set sensitivities,[43] the ^{t}Bu-methyl groups were represented by the standard double-ζ basis,[44] and polarization functions were included for the C atoms of the Cp rings ($\alpha_d = 0.75$). The unrestricted solutions for the quartet 15-electron or doublet 17-electron Cr compounds (agostic H atoms counted as dative ligands) display negligible spin-contamination. In contrast, the solution for a 15-electron doublet (**Iβ(²A)**) was significantly contaminated ($\langle \hat{S}^2 \rangle = 1.75$), and therefore the energy was corrected according to a scheme taking into account the contribution from the S+1 state.[46]

Acknowledgment. We thank Borealis Polymers Oy (Dr. O. Andell) for financial support and the Gesellschaft für wissenschaftliche Datenverarbeitung in Göttingen and the Max-Planck-Institute for Biological Cybernetics in Tübingen for computer facilities.

Supporting Information Available: Detailed information on the crystal structure determinations, including tables of data collection parameters, final atomic positional and thermal parameters, and interatomic distances and angles as well as ORTEP diagrams. This material is available free of charge via the Internet at http://pubs.acs.org.

OM010146M

(41) Frisch, M. J.; Trucks, G. W.; Schlegel, H. B.; Scuseria, G. E.; Robb, M. A.; Cheeseman, J. R.; Zakrzewski, V. G.; Montgomery, J. A., Jr.; Stratmann, R. E.; Burant, J. C.; Dapprich, S.; Millam, J. M.; Daniels, A. D.; Kudin, K. N.; Strain, M. C.; Farkas, O.; Tomasi, J.; Barone, V.; Cossi, M.; Cammi, R.; Mennucci, B.; Pomelli, C.; Adamo, C.; Clifford, S.; Ochterski, J.; Petersson, G. A.; Ayala, P. Y.; Cui, Q.; Morokuma, K.; Malick, D. K.; Rabuck, A. D.; Raghavachari, K.; Foresman, J. B.; Cioslowski, J.; Ortiz, J. V.; Baboul, A. G.; Stefanov, B. B.; Liu, G.; Liashenko, A.; Piskorz, P.; Komaromi, I.; Gomperts, R.; Martin, R. L.; Fox, D. J.; Keith, T.; Al-Laham, M. A.; Peng, C. Y.; Nanayakkara, A.; Gonzalez, C.; Challacombe, M.; Gill, P. M. W.; Johnson, B.; Chen, W.; Wong, M. W.; Andres, J. L.; Gonzalez, C.; Head-Gordon, M.; Replogle, E. S.; Pople, J. A. *Gaussian 98*, Revision A.7; Gaussian, Inc.: Pittsburgh, PA, 1998.

(42) Jensen, V. R.; Børve, K. J. *Organometallics* **1997**, *16*, 2514.

(43) Jensen, V. R.; Børve, K. J. *J. Comput. Chem.* **1998**, *19*, 947.

(44) Dunning, T. H.; Hay, P. J. In *Methods of Electronic Structure Theory*; Schaefer, H. F., Ed.; Plenum Press: New York, 1977; p 1.

(45) Hehre, W. J.; Stewart, R. F.; Pople, J. A. *J. Chem. Phys.* **1969**, *51*, 2657.

(46) Yamaguchi, K.; Jensen, F.; Dorigo, A.; Houk, K. N. *Chem. Phys. Lett.* **1988**, *149*, 537.